A Robust Method for ECG-Based Estimation of the Respiratory Frequency During Stress Testing

Raquel Bailón* , Leif Sörnmo, *Senior Member, IEEE*, and Pablo Laguna, *Senior Member, IEEE*

***Abstract*—A robust method is presented for electrocardiogram (ECG)-based estimation of the respiratory frequency during stress testing. Such ECGs contain highly nonstationary noise and exhibit changes in QRS morphology which, when combined with the dynamic nature of the respiratory frequency, make most existing methods break down. The present method exploits the oscillatory pattern of the rotation angles of the heart's electrical axis as induced by respiration. The series of rotation angles, obtained from least-squares loop alignment, is subject to power spectral analysis and estimation of the respiratory frequency. Robust techniques are introduced to handle the nonstationary properties of exercise ECGs. The method is evaluated by means of both simulated signals, and ECG/airflow signals recorded from 14 volunteers and 20 patients during stress testing. The resulting respiratory frequency estimation error is, for simulated signals, equal to 0.5% $\pm$ 0.2%, mean $\pm$ SD (0.002 $\pm$ 0.001 Hz), whereas the error between respiratory frequencies of the ECG-derived method and the airflow signals is 5.9% $\pm$ 4% (0.022 $\pm$ 0.016 Hz). The results suggest that the method is highly suitable for analysis of noisy ECG signals recorded during stress testing.**

***Index Terms*—ECG-derived respiration (EDR), electrocardiography, exercise, respiratory frequency, repiratory system, robustness, signal synthesis.**

I. Introduction

THE respiratory signal is usually recorded with techniques like spirometry, pneumography, or plethysmography. These techniques require the use of cumbersome devices that may interfere with natural breathing, and which are unmanageable in certain applications such as ambulatory monitoring, stress testing, and sleep studies. Nonetheless, the joint study of the respiratory and cardiac systems is of great interest in these applications and the use of methods for indirect extraction of respiratory information is particularly attractive to pursue. An important motivation of this study is to analyze the influence of the respiratory system in heart rate variability (HRV) during stress testing, since it has been observed that the power in the very high frequency band (0.4–1 Hz) exhibits potential value in coronary artery disease diagnosis [1], and HRV power spectrum distribution is likely to be dependent on respiratory frequency.

Manuscript received April 20, 2005; revised November 12, 2005. This work was supported by the Ministerio de Ciencia y Tecnología under Project TEC2004-05263-C02-02/TCM and Project SAB 2003-0130 and in part by the Diputación General de Aragón (DGA), Spain, through Grupos Consolidados GTC T30. *Asterisk indicates corresponding author.*

*R. Bailón is with the Communications Technology Group, Aragón Institute of Engineering Research (I3A), University of Zaragoza, María de Luna 1, 50015 Zaragoza, Spain (e-mail: rbailon@unizar.es).

L. Sörnmo, is with the Signal Processing Group, Department of Electroscience, Lund University, S-221 00 Lund, Sweden (e-mail: leif.sornmo@es.lth.se).

P. Laguna is with the Communications Technology Group, Aragón Institute of Engineering Research (I3A), University of Zaragoza, 50015 Zaragoza, Spain (e-mail: laguna@unizar.es).

Digital Object Identifier 10.1109/TBME.2006.871888

It is well-known that the respiratory activity influences electrocardiographic measurements in various ways. During the respiratory cycle, chest movements and changes in the thorax impedance distribution due to filling and emptying of the lungs cause a rotation of the electrical axis of the heart which affects beat morphology. The effect of respiration-induced heart displacement on the electrocardiogram (ECG) was first studied by Einthoven *et al.* [2] and quantified in further detail in [3] and [4]. Furthermore, respiration modulates heart rate (HR) such that it increases during inspiration and decreases during expiration [5]. It has also been shown that the mechanical action of respiration results in the same kind of frequency content in the ECG spectrum as does HRV [6].

Several studies have developed signal processing techniques to extract respiratory information from the recorded ECG, so-called ECG-derived respiratory (EDR) information. Some techniques are based on respiration-induced variations in beat-to-beat morphology [7]–[19], while others attempt to extract respiratory information from the HR [20]–[23].

The first EDR method based on morphologic variations dates back to 1974 when Wang *et al.* [7] proposed a model for the mechanics of the heart with respect to respired air volume of the lungs, and a technique for monitoring respiratory rate and depth using the vectorcardiogram (VCG). The respiratory activity was measured in terms of rotation of the intrinsic components of the VCG [24], as computed from the last 30 ms of the QR segment in every heartbeat. Later, Pinciroli *et al.* [8] and Moody *et al.* [25] proposed algorithms which exploit variations in the direction of the electrical axis. The electrical axis was calculated as the least-squares (LS) straight line which fits the projection of the VCG on the plane defined by two leads [8]. The variations of the angle between the electrical axis and a reference direction was defined as an EDR signal. Alternatively, the ratio of the QRS areas in two leads was used as a measure of respiratory activity [25]; this measure was later applied in HRV analysis [10] and sleep studies [15]. Using a similar principle, the area of the QRS complexes in eight leads was used to define an EDR signal [12]. First, an eight-dimensional (8-D) space was defined by eigenvalue analysis of a learning set, and then, each 8-D QRS area vector was projected onto the main direction, which was considered as particularly sensitive to respiratory information. For single lead recordings, amplitude modulation of ECG waves has been used to derive a respiratory signal [11], [], [14], [17], [], as well as direct filtering of the ECG in the usual respiratory frequency band [16]. Recently, the respiratory frequency was obtained as the dominant frequency of the estimated rotation angles of the electrical axis [18]. Estimation of the rotation angles of the electrical axis was accomplished by spatiotemporal alignment of successive QRS-VCG loops with respect to a reference loop. Variations in QRS-VCG loop morphology were also

used to estimate the respiratory signal [19]; principal component analysis was applied to measurements on center of gravity and inertial axes of each loop, and the first principal component was identified as the respiratory activity.

Some methods derive respiratory information solely from the HR series. The respiratory frequency was estimated from the RR interval series using singular value decomposition (SVD) to track the most important instantaneous frequencies of the interval series [21]. This method performed well in ECGs recorded during rest and in tilt ECGs but failed during exercise. Some years later, the respiratory frequency present in the HR series was derived using the S-transform, being a continuous wavelet transform with phase correction [22]. Recently, respiratory frequency patterns were derived from the RR interval series during pyramidal exercise, using an AR model-based method to track the respiratory frequency [23].

In 1990, Varanini introduced a method for deriving a respiratory signal which combined beat morphology and HR information [20]. The R-wave amplitude of a single lead and the RR interval time series were used as input to an adaptive filter whose output was an EDR signal. In a recent study, a method combining ECG morphology and HR was, however, found to perform worse than a method involving only morphology [18].

Although the ECG is often recorded during noisy conditions, marginal attention has been paid to the development of robust EDR methods. Signals recorded during stress testing are highly nonstationary and noisy, mainly due to muscular activity and motion artifacts. Moreover, the respiratory frequency during exercise is in itself a highly dynamic quantity and changes with effort and work load.

The aim of our work is twofold: first, to develop a robust method for estimation of the respiratory frequency in noisy recordings; second, to evaluate the performance using respiratory signals recorded simultaneously by an airflow thermistor. The method described in this paper considerably extends the one described in [18] by better accounting for the special characteristics of exercise ECGs. Section II presents the different stages of the method, namely, signal preprocessing, EDR signal estimation, respiratory frequency estimation by spectral analysis, and two robustifying techniques [outlier correction/rejection and beat substitution in leads with poor signal-to-noise ratio (SNR)]. In Section III, the data sets for performance evaluation are described. A simulation study is designed which accounts for nonstationary properties of the ECG, noise and respiration during exercise. The performance is also evaluated on exercise ECGs by comparing the results with those obtained from simultaneously recorded respiratory signals. The performance measures are described in Section IV, and applied in Section V to evaluate the performance on both simulated and real signals, and compared to the performance of the multilead QRS area method [25].

II. Methods

A. Signal Preprocessing

QRS complexes are detected and clustered based on their morphology; only beats with the dominant morphology are analyzed in the following. Baseline wander is attenuated using the cubic splines method. The VCG is synthesized by means of the inverse Dower transformation [26].

B. EDR Algorithm

Estimation of the rotation angles of the electrical axis is based on the fact that successive QRS-VCG loops have similar morphology but slightly different direction in space during the respiratory cycle relative to a reference QRS-VCG loop [18]. The EDR signal is defined by the series of LS rotation angle estimates between successive loops and the reference loop.

The method performs minimization of a normalized distance ε between a reference loop ($N \times 3$ matrix $\mathbf{Y_R}$, where the columns contain the X, Y, and Z leads) and each observed loop ($(N+2\Delta) \times 3$ matrix $\mathbf{Y}$), with respect to rotation (3×3 matrix $\mathbf{Q}$), amplitude scaling (scalar γ), and time synchronization ($N \times (N+2\Delta)$ matrix $\mathbf{J}_\tau$) [27], [28]

$$\varepsilon_{\min} = \min_{\gamma,\tau,\mathbf{Q}}(\varepsilon) = \min_{\gamma,\tau,\mathbf{Q}} \frac{\|\mathbf{Y_R} - \gamma \mathbf{J}_\tau \mathbf{Y} \mathbf{Q}\|_F^2}{\|\gamma \mathbf{J}_\tau \mathbf{Y} \mathbf{Q}\|_F^2} \tag{1}$$

where

$$\mathbf{J}_\tau = [\mathbf{0}_{\Delta-\tau} \quad \mathbf{I} \quad \mathbf{0}_{\Delta+\tau}] \tag{2}$$

and N is the number of samples of the QRS complex analysis window. The parameter Δ denotes the number of symmetrically augmented samples which allow for time synchronization with $\tau = -\Delta, \ldots, \Delta$. The dimensions of the $\mathbf{0}_{\Delta-\tau}$, $\mathbf{0}_{\Delta+\tau}$, and $\mathbf{I}$ (identity) matrices are $N \times (\Delta - \tau)$, $N \times (\Delta + \tau)$, and $N \times N$, respectively. The operator $\|\cdot\|_F^2$ denotes the Frobenius norm.

The rotation matrix $\mathbf{Q}$ can be viewed as three successive rotations around each axis (lead), defined by the rotation angles ϕ_X, ϕ_Y, and ϕ_Z

$$\mathbf{Q} = \begin{bmatrix} 1 & 0 & 0 \\ 0 & \cos(\phi_X) & \sin(\phi_X) \\ 0 & -\sin(\phi_X) & \cos(\phi_X) \end{bmatrix} \begin{bmatrix} \cos(\phi_Y) & 0 & \sin(\phi_Y) \\ 0 & 1 & 0 \\ -\sin(\phi_Y) & 0 & \cos(\phi_Y) \end{bmatrix} \times \begin{bmatrix} \cos(\phi_Z) & \sin(\phi_Z) & 0 \\ -\sin(\phi_Z) & \cos(\phi_Z) & 0 \\ 0 & 0 & 1 \end{bmatrix}. \tag{3}$$

The normalized distance ε is minimized by first finding the estimates of γ and $\mathbf{Q}$ for every value of τ and then selecting that τ for which ε is minimum. For a fixed τ, the optimal estimator of $\mathbf{Q}$ is given by [27]

$$\hat{\mathbf{Q}}_\tau = \mathbf{V}_\tau \mathbf{U}_\tau^T \tag{4}$$

where the matrices $\mathbf{U}_\tau$ and $\mathbf{V}_\tau$ contain the left and right singular vectors from the SVD of $\mathbf{Z}_\tau = \mathbf{Y}_\mathbf{R}^T \mathbf{J}_\tau \mathbf{Y}$. The estimate of γ is obtained by [28]

$$\hat{\gamma}_\tau = \frac{tr\left(\mathbf{Y}_\mathbf{R}^T \mathbf{Y}_\mathbf{R}\right)}{tr\left(\mathbf{Y}_\mathbf{R}^T \mathbf{J}_\tau^T \mathbf{Y} \hat{\mathbf{Q}}_\tau\right)}. \tag{5}$$

The parameters $\hat{\mathbf{Q}}_\tau$ and $\hat{\gamma}_\tau$ are calculated for all values of τ, with $\hat{\mathbf{Q}}$ resulting from that τ which yields the minimal error ε. Finally, the rotation angles ϕ_X, ϕ_Y, and ϕ_Z are derived from $\hat{\mathbf{Q}}$ using the structure in (3), see [18].

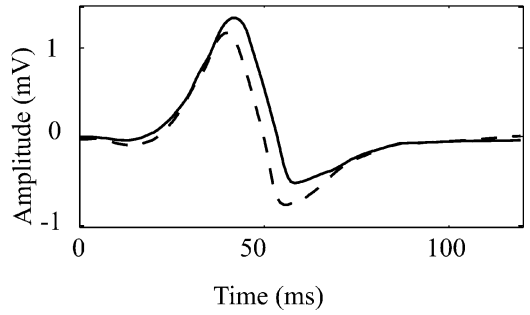

Fig. 1. Reference loop (lead X) at onset (solid line) and peak exercise (dashed line) of a stress test.

During exercise, QRS morphology is influenced by exercise-induced ST changes. To reduce such influence on the angle estimates, an exponentially updated reference loop is introduced

$$\mathbf{Y_R}(i+1) = \alpha \mathbf{Y_R}(i) + (1-\alpha)\mathbf{Y}(i+1) \tag{6}$$

where i denotes the beat index at time instant t_i (i.e., $\mathbf{Y_R}(t_i) = \mathbf{Y_R}(i)$ and $\mathbf{Y}(t_i) = \mathbf{Y}(i)$). The parameter α is chosen such that morphologic variation is tracked while adaptation to noise is avoided. The initial reference loop $\mathbf{Y_R}(1)$ is defined as the average of the first ten loops, on condition that all loops have crosscorrelation coefficients with the first loop that exceed 0.9 in all leads. Fig. 1 displays lead X of $\mathbf{Y_R}$ at the beginning and peak exercise of a stress test, and illustrates the extent by which QRS morphology may change during exercise.

The QRS complex analysis window comprises 120 ms centered around the QRS mark, and it is symmetrically augmented by 30 ms to allow time synchronization in steps of 1 ms. A forgetting factor of $\alpha = 0.8$ is used in the present study.

C. Estimation of Respiratory Frequency

The respiratory frequency is estimated from the location of the largest peak in a running average of the power spectrum obtained from the EDR signals $\phi_X(t_i)$, $\phi_Y(t_i)$, and $\phi_Z(t_i)$. The estimation procedure is divided into two parts—estimation of power spectrum and peak location—which both are aimed at robust performance.

Estimation of the power spectrum is accomplished with Lomb's method [29] because the samples of the EDR signals are unequally spaced and may contain gaps in noisy and ectopic periods. Individual running power spectra of each EDR signal are averaged in order to reduce the variance; for the j^{th} lead and k^{th} running interval of T_s-s length, the power spectrum $S_{j,k}(f)$ results from averaging the power spectra obtained from subintervals of length T_m s ($T_m < T_s$) using an overlap of $T_m/2$ s. A T_s-s spectrum is estimated every t_s s. The variance of $S_{j,k}(f)$ is further reduced by "peak-conditioned" averaging in which selective averaging is performed only on those $S_{j,k}(f)$ which are sufficiently peaked. In this paper, "peaked" is synonymous to that a certain percentage (ξ) of the spectral power must be contained in an interval centered around the largest peak $f_p(j,k)$, otherwise the spectrum is omitted from averaging. In mathematical terms, peak-conditioned averaging is defined by

$$\overline{S}_k(f) = \sum_{l=0}^{L_s-1} \sum_{j\in\{\text{X,Y,Z}\}} \chi_{j,k-l} S_{j,k-l}(f), \quad k = 1,2,\ldots \tag{7}$$

where the parameter L_s denotes the number of T_s-s intervals used for computing the averaged spectrum $\overline{S}_k(f)$. The binary variable $\chi_{j,k}$ indicates if the spectrum $S_{j,k}(f)$ is peaked or not, defined by

$$\chi_{j,k} = \begin{cases} 1, & P_{j,k} \geq \xi \\ 0, & \text{otherwise} \end{cases} \tag{8}$$

where the relative spectral power $P_{j,k}$ is given by

$$P_{j,k} = \frac{\int_{(1-g)f_p(j,k)}^{(1+g)f_p(j,k)} S_{j,k}(f)df}{\int_{0.1}^{f_{\max}(k)} S_{j,k}(f)df} \tag{9}$$

the value of $f_{\max}(k)$ is given by the minimum between 0.9 Hz and half the mean HR in the k^{th} interval, and g determines the width of integration interval.

Fig. 2(a) illustrates the estimation of the power spectrum $S_{X,k}(f)$ using different values of T_m. It can be appreciated that larger values of T_m yield spectra with better resolution and, therefore, more accurate estimation of the respiratory frequency. However, the respiratory frequency does not always correspond to a unimodal peak (i.e., showing a single frequency peak), but sometimes to a bimodal peak, especially during exercise. In such situations, smaller values of T_m should be used to estimate the gross dominant frequency.

Estimation of the respiratory frequency $\hat{f}(k)$ as the largest peak of $\overline{S}_k(f)$ comes with the risk of choosing the location of a spurious peak. This risk is, however, considerably reduced by narrowing down the search interval to only include frequencies in an interval of 2δ Hz centered around a reference frequency $f_w(k) : [f_w(k) - \delta, f_w(k) + \delta]$. The reference frequency is obtained as an exponential average of previous estimates, using

$$f_w(k+1) = \beta f_w(k) + (1-\beta)\hat{f}(k) \tag{10}$$

where β denotes the forgetting factor.

The following parameter values are used: $T_s = 40$ s, so as to obtain a reliable estimation of the lowest expected respiratory frequency (considered here at 0.15 Hz) while handling the nonstationary nature of respiratory frequency, $t_s = 5$ s, so as to track changes in respiratory frequency assuming that they never occur faster than 5 s, and $L_s = 5$, so as to reduce the variance of the spectral estimation assuming that respiration can be considered stationary in 60-s intervals (L_s overlapped T_s-s spectra comprise a total interval of 60 s); the value $T_m = 12$ s yields the minimum mean intrasubject estimation error [see Table II and Fig. 9(a)]; $g = 0.5$ and $\xi = 0.35$ are used based on the observation of rotation angle spectra; $\beta = 0.7$ is used based on real respiratory patterns during stress testing and $\delta = 0.2$ Hz assuming that respiratory frequency variations are not faster than 0.2 Hz per 5 s; finally, $f_w(1) = \arg \max_{0.15 \leq f \leq 0.4} (\overline{S}_1(f))$ so as to reduce the risk of spurious frequency selection in the initialization of (10). In the simulation study, the parameter T_m is assigned a different value ($T_m = T_s = 40$ s) since the simulated respiratory frequency always corresponds to a unimodal peak.

The procedure to estimate the respiratory frequency is summarized in Fig. 2(b).

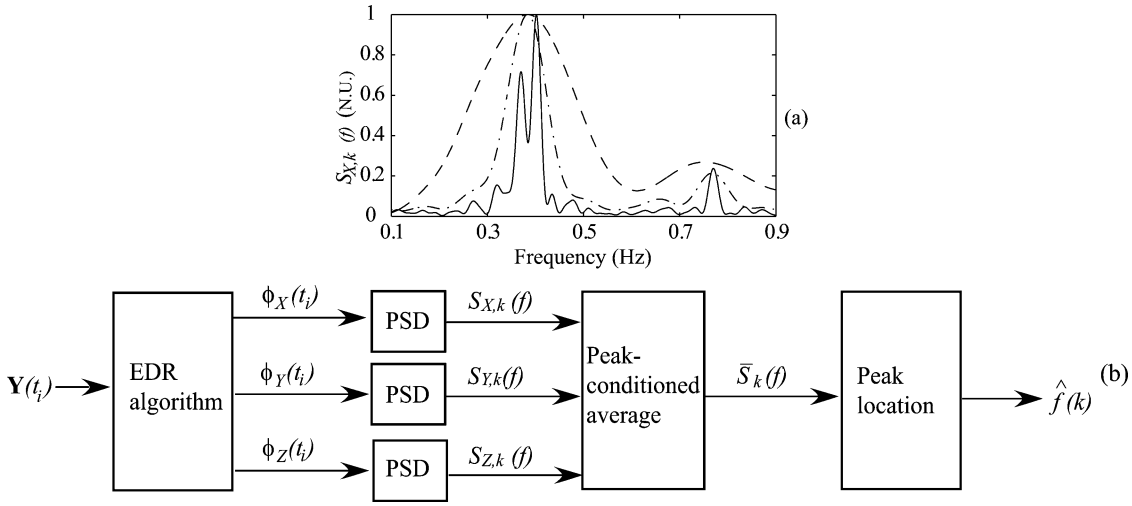

Fig. 2. (a) Power spectrum $S_{X,k}(f)$ computed for $T_m = 4$ s (dashed line), 12 s (dashed/dotted line) and 40 s (solid line), using $T_s = 40$ s. (b) Block diagram of the estimation of respiratory frequency.

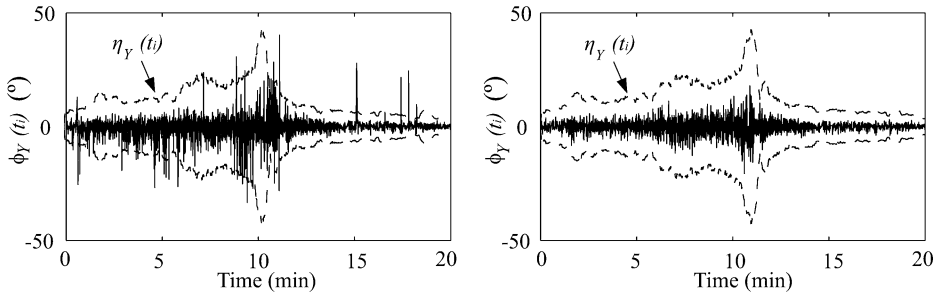

Fig. 3. EDR signal $\phi_Y(t_i)$ estimated before (left) and after (right) outlier correction/rejection. Dashed lines denote the running threshold $\eta_Y(t_i)$.

D. Outlier Correction/Rejection

Unreliable angle estimates are sometimes observed at poor SNRs or in the presence of ectopic beats. Such outlier estimates are detected when the absolute value of the angle estimates exceed a lead-dependent threshold $\eta_j(t_i)$ ($j \in \{\mathrm{X}, \mathrm{Y}, \mathrm{Z}\}$). The threshold $\eta_j(t_i)$ is defined as the running standard deviation (SD) of the N_e most recent angle estimates, multiplied by a factor C. For $i < N_e$, $\eta_j(t_i)$ is computed from the available estimates. Outliers are replaced by the angle estimates obtained by reperforming the minimization in (1), but excluding the value of τ which resulted in the outlier estimate. The new estimates are only accepted if they do not exceed the threshold $\eta_j(t_i)$; if no acceptable value of τ is found, the EDR signal will contain a gap and the reference loop $\mathbf{Y_R}$ in (6) will not be updated. The correction/rejection procedure is illustrated by Fig. 3 for angle estimates related to lead Y. The values of the parameters N_e and C are chosen as a compromise between correcting or rejecting outlier angle estimates and allowing changes in maximum rotation angle values during stress testing. Different values of N_e (25, 50, 75, 100) and C (1, 3, 5, 7) have been tested, being the couple $N_e = 50$, $C = 5$ the one yielding the minimum mean intrasubject estimation error.

E. Beat Substitution in Leads With Poor SNR

To further reduce the presence of outlier estimates, noisy beats are substituted on a lead-by-lead basis using an exponentially updated average beat [see (6)]. The rationale behind this rule is that excessive noise present in a single lead masks the rotation information since the noise influences, to various extents, all three synthesized VCG leads. Beat substitution is therefore performed on the 12-lead ECG rather than on the VCG so that rotation information can still be present in all VCG leads even if it has been removed from some of the 12 leads. If beat substitution were done directly in the VCG, rotation information coming from some acceptable 12-leads would be lost.

Two different kinds of noise are common in exercise ECGs: high-frequency (HF) noise mainly due to muscle activity, and low-frequency (LF) noise due to remaining baseline wander that could not be attenuated by the preprocessing described in Section II-A. Consequently, a high-frequency SNR, $\mathrm{SNR_{HF}}$, and a low-frequency SNR, $\mathrm{SNR_{LF}}$, are defined to determine beats for substitution. The $\mathrm{SNR_{HF}}$ is defined as the ratio of the peak-to-peak amplitude in an interval centered around the QRS mark, and the root-mean-square (RMS) value of the HF noise (using a Butterworth filter with cut-off frequency f_c Hz) in a HR-dependent interval after the QRS mark. The $\mathrm{SNR_{LF}}$ is defined as the ratio of the peak-to-peak amplitude of the exponentially updated average beat and the RMS value of the residual ECG after average beat substraction and low-pass filtering (using a Butterworth filter with cut-off frequency f_c Hz). Beats whose $\mathrm{SNR_{HF}}$ is below a threshold η_{HF} or whose $\mathrm{SNR_{LF}}$ is below a threshold η_{LF} are substituted by their corresponding averaged beats. Fig. 4 displays a synthesized VCG before and after substitution of noisy beats, as well as the EDR signals estimated from them and the airflow-based respiratory signal. The

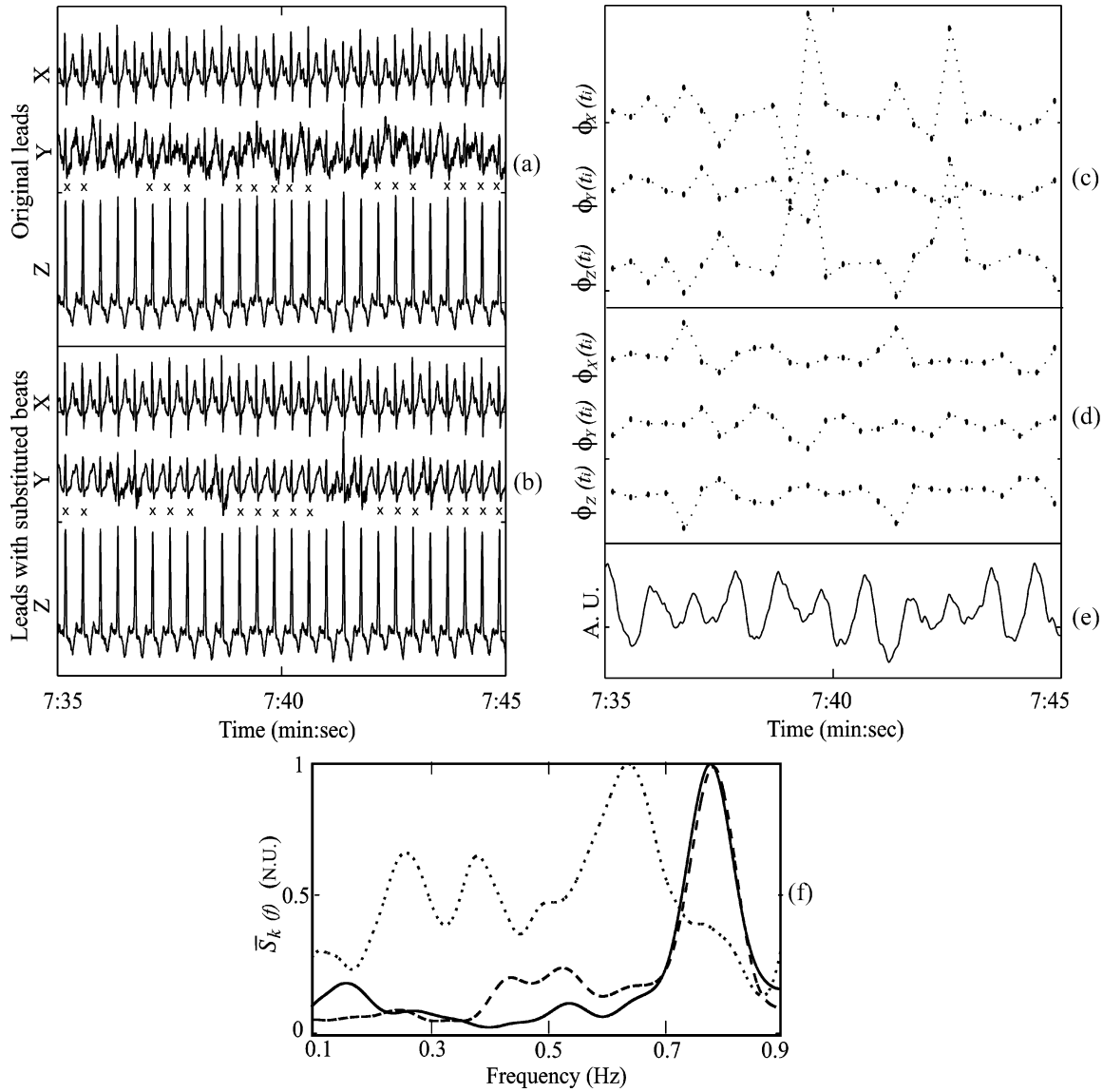

Fig. 4. VCG leads (a) before and (b) after substitution of noisy beats. Substituted beats in lead Y have been marked (×). The EDR signals estimated (c) before and (d) after substitution of noisy beats, and (e) the related respiratory signal. (f) Power spectrum of the respiratory signal (solid line), and the EDR signals before (dotted line) and after (dashed line) substitution of noisy beats.

spectra obtained from the EDR signals and the respiratory signal are also displayed in Fig. 4. It is obvious that the substitution of noisy beats improves the estimation of the respiratory frequency since the largest peak of the EDR spectrum has been shifted and it coincides with the largest peak of the respiratory spectrum. The parameter values used are: $f_c = 20$ Hz, $\eta_{\mathrm{HF}} = 20$, $\eta_{\mathrm{LF}} = 3$, and $\alpha = 0.1$ in (6) to obtain the average beat.

F. Multilead QRS Area

For comparison, an EDR method based on QRS areas is implemented [25]. The ratio between the QRS areas in two orthogonal leads defines an angle θ resembling the direction of the electrical axis in relation to one of the leads

$$\begin{aligned} \theta_{XY} &= \arctan(A_Y/A_X) \\ \theta_{XZ} &= \arctan(A_Z/A_X) \\ \theta_{YZ} &= \arctan(A_Z/A_Y) \end{aligned} \tag{11}$$

where A_j $(j \in \mathrm{X}, \mathrm{Y}, \mathrm{Z}\})$ represents the QRS area computed by the trapezoidal method. The trends of $\hat{\theta}_{XY}(t_i)$, $\hat{\theta}_{XZ}(t_i)$, and $\hat{\theta}_{YZ}(t_i)$, resulting from each i^{th} QRS-VCG loop, are used as EDR signals. The QRS area is computed from 60 ms before to 20 ms after the QRS detection mark. The time interval is selected so as to reduce the influence of QRS morphologic variations induced by exercise. Signal preprocessing and estimation of the respiratory frequency are performed in the same way as for the QRS-VCG loop alignment and include beat substitution in leads with poor SNR.

III. Data Sets

A. Stress Test Data

The standard 12-lead ECG and an airflow-based respiratory signal were simultaneously recorded from 14 volunteers (10 males and 4 females, aged 28 ± 4 years) and 20 patients (16

males and 4 females, aged 58 ± 16 years), referred to the Department of Clinical Physiology at the University Hospital of Lund, Sweden, for stress testing.

The stress test was performed on a bicycle ergometer (Ergoline 900C, Siemens-Elema) during which the ECG was recorded using the Siemens-Elema Megacart front-end. The leads were digitized at a sampling rate of 1 kHz and amplitude resolution of 0.6 μV. The respiratory signal was recorded using an airflow thermistor (Sleepmate), amplified (DA100C, Biopac) and digitized (MA100, Biopac) at a sampling rate of 50 Hz. The bandpass filter cut-off frequencies were at 0.05 and 10 Hz, respectively.

During the stress test the initial workload (50 W for males and 30 W for females) was increased at a rate of 15 W/min for males and 10 W/min for females. Blood pressure, HR, and rate of perceived exertion (RPE, scored from 6 to 20 according to the Borg scale [30]) were monitored during the test, which ended when an RPE of 15 was reached for the volunteers, and as prescribed by clinical routine for the patients. Signals were recorded from the beginning of exercise until 4 min of recovery. However, the recovery phase was excluded in the evaluation of the method since once the exercise finished the subject moved from the ergometer to lay on the bed; as a result, respiratory signal from the thermistor is affected by motion artifacts which, in many cases, make it impossible to obtain a reliable reference respiratory frequency.

A total of five subjects, all of them patients, were excluded from the study. Three were automatically excluded because the spectra of the respiratory signal did not exhibit a dominant peak in at least 50% of the total duration of the exercise (two of them were referred for stress testing to check for angina pectoris, the remaining one underwent coronary bypass surgery). One subject was excluded because of unattached electrodes. Finally, one subject was excluded because the heart rate was too low to assure aliasing-free estimation of the respiratory frequency (this patient was referred for stress testing because of suspected myocardial ischemia). A total of 14 volunteers and 15 patients were included for performance evaluation.

B. Simulated Data

A simulation study is designed to evaluate the method in a situation where all signal parameters can be controlled. The study consists of a set of computer-generated reference exercise ECGs to which noise (mainly due to muscle activity and body movement) and respiratory influence have been added.

The simulated signals are based on the ECGs of 844 patients and 66 asymptomatic volunteers recorded in the University Hospital "Lozano Blesa" of Zaragoza, Spain, during treadmill stress testing. The standard leads (V1, V3-V6, I, II, III, aVR, aVL, and aVF) and RV4 were digitized at a sampling rate of 1 kHz and amplitude resolution of 0.6 μV.

First, a noise-free 12-lead ECG is simulated from a set of 15 beats (templates) extracted from rest, exercise, and recovery of a stress test using weighted averaging. The HR and ST depression of each template is modified to follow a predefined ST/HR pattern. The simulated signals result from concatenation of templates such that HR and ST depression evolve linearly with time.

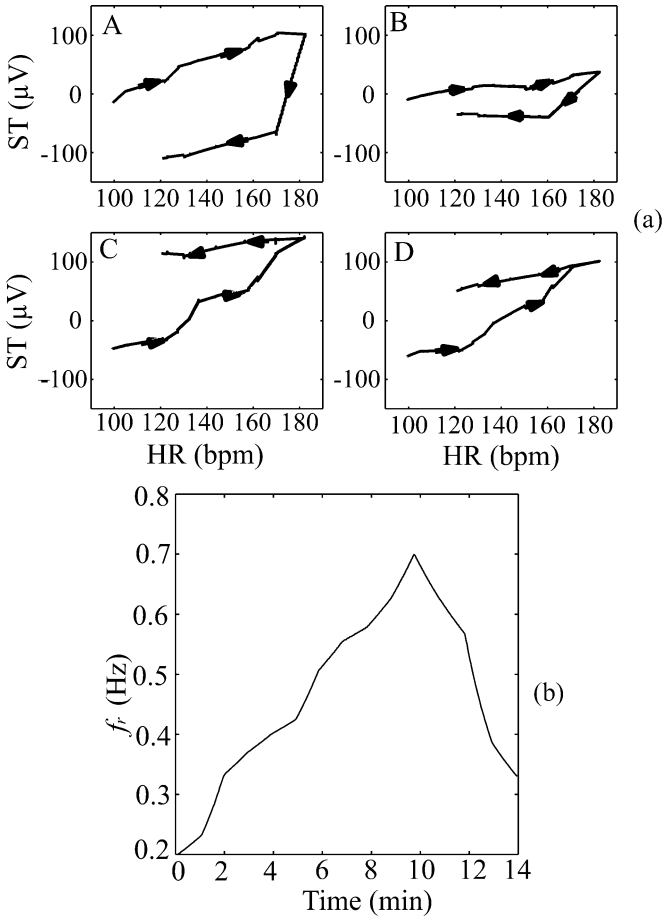

Fig. 5. (a) ST/HR patterns of simulated ECGs where ST depression is displayed versus HR. Note that the values on the vertical axis correspond to ST depression, not ST amplitude. Patterns A and B are typical for healthy subjects, whereas patterns C and D are typical for ischemic patients. (b) Simulated respiratory frequency pattern.

Four different ST/HR patterns based on actual cases are used, see Fig. 5(a). The ST depression is estimated at a HR-dependent distance from the QRS mark, see [1] for details.

The VCG signal is synthesized from the simulated 12-lead ECG using the same methodology as the inverse Dower transformation [26], but now modified to account for the spatial location of RV4 rather than the standard lead V2 [31].

In order to account for the respiratory influence, the simulated VCG is transformed on a sample-by-sample basis with a three-dimensional rotation matrix defined by time-varying angles. The angular variation around each axis is modeled by the product of two sigmoidal functions reflecting inhalation and exhalation [32], such that for lead X

$$\phi_X(n) = \sum_{p=0}^{\infty} \zeta_X \frac{1}{1+e^{-\lambda_i(p)(n-\kappa_i(p))}} \frac{1}{1+e^{\lambda_e(p)(n-\kappa_e(p))}},$$

$$\lambda_i(p) = 20\frac{f_r(p)}{f_s}, \quad \kappa_i(p) = \kappa_i(p-1) + \frac{f_s}{f_r(p-1)},$$

$$\kappa_i(0) = 0.35 f_s,$$

$$\lambda_e(p) = 15\frac{f_r(p)}{f_s}, \quad \kappa_e(p) = \kappa_e(p-1) + \frac{f_s}{f_r(p-1)},$$

$$\kappa_e(0) = 0.6 f_s \tag{12}$$

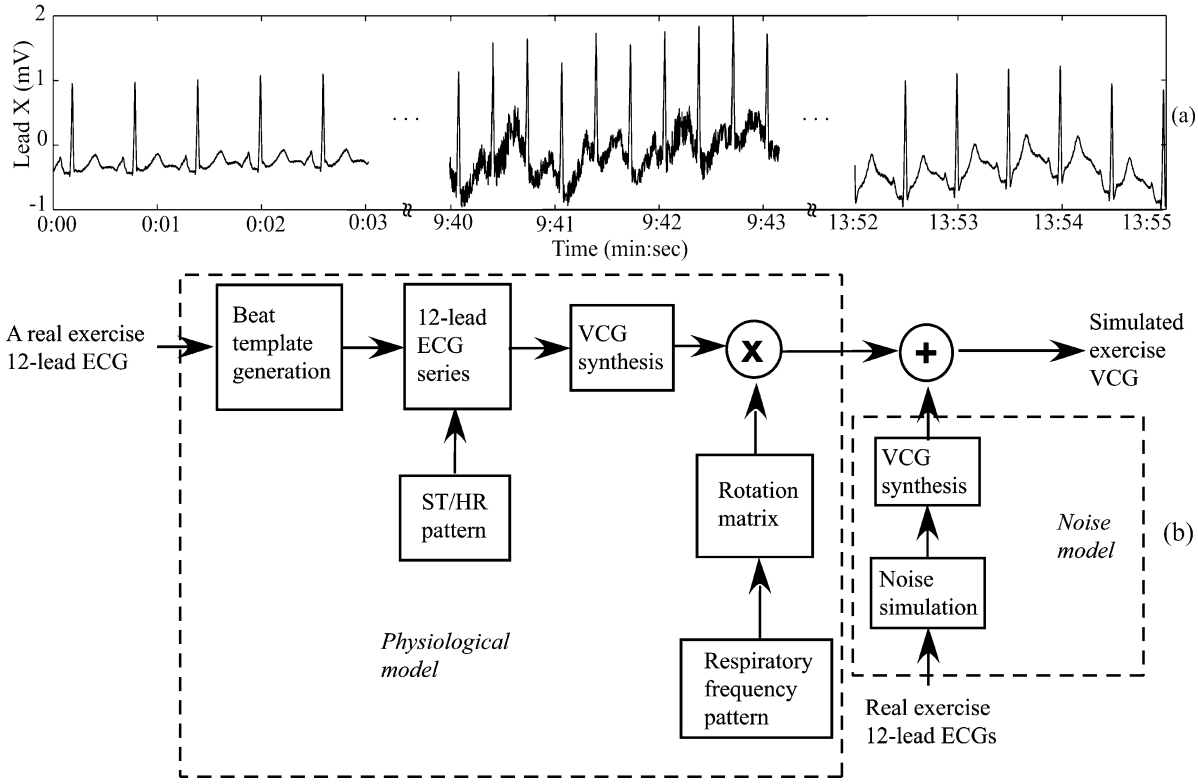

Fig. 6. (a) Simulated ECG signal at onset, peak exercise, and end of a stress test. (b) Block diagram of the simulation design. Note that the 12-lead ECGs used for signal and noise generation are different.

where n denotes sample index, p each respiratory cycle index, $1/\lambda_i(p)$ and $1/\lambda_e(p)$ are the duration of inhalation and exhalation, respectively, $\kappa_i(p)$ and $\kappa_e(p)$ the time delays of the sigmoidal functions, f_s the sampling rate, $f_r(p)$ the respiratory frequency, and ζ_X the maximum angular variation around lead X, which has been set to 5 in. The same procedure is applied to leads Y and Z, with $\zeta_Y = \zeta_Z = \zeta_X$. To account for the dynamic nature of the respiratory frequency during a stress test, the simulated respiratory frequency $f_r(p)$ follows a pattern varying from 0.2 to 0.7 Hz, see Fig. 5(b). A similar respiratory pattern has been observed in several of the stress tests collected for this study.

Finally, noise is added to the concatenated ECG signals, obtained as the residual between raw exercise ECGs and a running average of the heartbeats [1]. The noise contribution to the VCG is synthesized from the 12-lead noise records. A total of 25 different noise records are used.

In Fig. 6(a), lead X of a simulated VCG is displayed during different stages of a stress test. The simulation procedure is summarized in Fig. 6(b).

IV. Performance Measures

To evaluate the method, the respiratory frequency extracted from the exercise ECG is compared to that extracted from the respiratory signal, simultaneously recorded as described in Section III-A. To obtain the reference frequency, $\hat{f}_r(k)$, spectral analysis, parallel to the one described in Section II-C, is applied to the respiratory signal (the only difference being that ξ is set to 75% since respiratory spectra are more peaky than angle spectra).

An absolute and a relative error trend are defined for each subject q at those indexes k where both estimates, $\hat{f}(k)$ and $\hat{f}_r(k)$, are available

$$\Delta f_q(k) = \left|\hat{f}_q(k) - \hat{f}_{r,q}(k)\right| \tag{13}$$

$$\Delta f_{q\%}(k) = \frac{\left|\hat{f}_q(k) - \hat{f}_{r,q}(k)\right|}{\hat{f}_{r,q}(k)} \times 100(\%) \tag{14}$$

where k, thus, indexes the averaged spectrum $\overline{S}_k(f)$ from which $\hat{f}(k)$ is estimated.

For each subject q, the mean and SD of the error trends characterize the intrasubject error. The mean intrasubject error is defined by the pair (μ, σ)

$$\mu = \frac{1}{S}\sum_{q=1}^{S}\frac{1}{N_q}\sum_{k=1}^{N_q}\Delta f_q(k) \tag{15}$$

$$\sigma^2 = \frac{1}{S}\sum_{q=1}^{S}\frac{1}{N_q-1} \times \sum_{k=1}^{N_q}\left(\Delta f_q(k) - \frac{1}{N_q}\sum_{k=1}^{N_q}\Delta f_q(k)\right)^2 \tag{16}$$

where N_q is the number of averaged spectra in which respiratory frequency could be estimated from both the ECG and the respiratory signal and S is the number of subjects. The parameters μ and σ represent the mean and SD, respectively, of the error trend, averaged among all subjects. The parameter $T_{\%}$ is computed as the average among all subjects of the percentage of

the total duration of exercise when respiratory frequency could be estimated from both the ECG and the respiratory signal.

The mean intrasubject error (μ, σ) is then compared to the mean intrasubject short-term variability of the respiratory frequency (μ_r, σ_r) during the stress test. For each subject q, the SD of $\hat{f}_{r,q}(k)$ (denoted as $v_{r,q}(l)$) is estimated over overlapping T_l-s intervals, offset by t_l s

$$v_{r,q}^2(l) = \frac{1}{M_{l,q}-1} \sum_{m=l-M_{l,q}/2+1}^{l+M_{l,q}/2} \left(\hat{f}_{r,q}(m) - \frac{1}{M_{l,q}} \times \sum_{k=l-M_{l,q}/2+1}^{l+M_{l,q}/2} \hat{f}_{r,q}(k) \right)^2. \quad (17)$$

Then, the mean intrasubject short-term variability is defined by

$$\mu_r = \frac{1}{S} \sum_{q=1}^{S} \frac{1}{L_q} \sum_{l=1}^{L_q} v_{r,q}(l) \quad (18)$$

$$\sigma_r^2 = \frac{1}{S} \sum_{q=1}^{S} \frac{1}{L_q - 1} \sum_{l=1}^{L_q} \left(v_{r,q}(l) - \frac{1}{L_q} \sum_{l=1}^{L_q} v_{r,q}(l) \right)^2. \quad (19)$$

The parameter $M_{l,q}$ is the number of estimates of $\hat{f}_{r,q}(k)$ within the l^{th} T_l-s interval, and L_q is the number of intervals offset by t_l s in which the series $v_{r,q}(l)$ has been segmented. The series $v_{r,q}(l)$ stands for the short-term (T_l-s) variability of the airflow-based respiratory frequency (reference frequency) for a subject q. The parameters μ_r and σ_r represent the mean and SD, respectively, of the short-term variability series, averaged among all subjects. The parameter values used are: $T_l = 60$ s, $t_l = 5$ s, so as the short-term variability series $v_{r,q}(l)$ has the same sampling and resolution as the error trend $\Delta f_q(k)$.

The validation in the simulation study is performed in a similar manner, however, the reference frequency, f_r, is already known. The parameter q denotes different realizations over the same deterministic rotation angle series, S denotes the number of realizations or simulated ECGs, and $T_{\%}$ denotes the percentage of the total time when the respiratory frequency could be estimated, averaged among all realizations. The mean, $\overline{f}(k)$, and SD, $\sigma_f(k)$, trends of the respiratory frequency estimated overall the realizations are defined by

$$\overline{f}(k) = \frac{1}{S} \sum_{q=1}^{S} \hat{f}_q(k), \quad \sigma_f^2(k) = \frac{1}{S-1} \sum_{q=1}^{S} \left(\hat{f}_q(k) - \overline{f}(k) \right)^2. \quad (20)$$

V. Results

A. Simulated Data

The method is evaluated on a total of 100 simulated ECGs, resulting from the combination of the four different ST/HR patterns and the 25 noise records.

The mean and SD of the intrasubject error on the simulated data are shown in Table I(a). The trends $\overline{f}(k)$ and $\sigma_f(k)$ are displayed in Fig. 7, showing that QRS-VCG loop alignment exhibits considerably more robust performance during the latter phase of exercise.

TABLE I
MEAN ± SD OF THE INTRASUBJECT ERROR. (a) SIMULATED DATA; (b) STRESS TEST DATA; (c) VOLUNTEERS VERSUS PATIENTS IN QRS-VCG LOOP

(a)

	QRS-VCG loop		Multi-lead QRS area	
	μ	σ	μ	σ
Hz	0.002 ± 0.001	0.003 ± 0.004	0.005 ± 0.004	0.009 ± 0.012
%	0.5 ± 0.2	0.7 ± 0.8	1.0 ± 0.7	1.7 ± 2.0
$T_{\%}$	96±2		95±3	

(b)

	QRS-VCG loop		Multi-lead QRS area	
	μ	σ	μ	σ
Hz	0.022 ± 0.016	0.028 ± 0.018	0.076 ± 0.087	0.056 ± 0.029
%	5.9 ± 4.0	7.6 ± 4.1	18.8 ± 21.7	14.9 ± 8.9
$T_{\%}$	78±17		58±19	

(c)

	Volunteers		Patients	
	μ	σ	μ	σ
Hz	0.016 ± 0.009	0.020 ± 0.009	0.028 ± 0.018	0.035 ± 0.021
%	4.7 ± 2.9	6.0 ± 3.1	7.0 ± 4.7	9.0 ± 4.4
$T_{\%}$	82±15		75±17	

B. Stress Test Data

The proposed method is applied to exercise ECGs and yields the results presented in Table I(b).

The intrasubject short-term variability of the reference frequency across all the subjects is $\mu_r = 0.019 \pm 0.007$ Hz (5.2% ± 1.9%) and $\sigma_r = 0.012 \pm 0.004$ Hz (3.3% ± 1.4%). Fig. 8 displays the respiratory frequency estimated from the respiratory signal ($\hat{f}_r(k)$) and from the ECG ($\hat{f}(k)$) for a volunteer and for a patient. Fig. 8(a) displays lead X of the observed and reference loop at different time instants during the stress test.

To study the influence of T_m (see Section II-C) on the estimation of the respiratory frequency, the mean ± SD of the intrasubject error (μ and σ) was calculated for different values of T_m, see Fig. 9(a) and Table II.

The value $T_m = 12$ s achieves the lowest mean intrasubject error in our study population. A lower value of T_m increases the mean error but decreases its SD due to the implicit spectral averaging, whereas a higher value of T_m increases both the mean and the SD of the error.

In this paper, two robustifying techniques are introduced to handle exercise ECGs. To assess the improvement achieved by each of the techniques, the basic method comprising signal preprocessing, EDR algorithm, and estimation of respiratory frequency [Section II-A–II-C] is first evaluated; then, the two robustifying techniques are evaluated by sequentially adding them to the basic method. The mean ± SD of the intrasubject error (μ) in each step is displayed in Fig. 9(b). The correction/rejection of outlier angle estimates reduces the mean intrasubject error from $\mu = 0.050$ Hz (12.1%) to $\mu = 0.030$ Hz (6.8%), and beat substitution further decreases the error to $\mu = 0.022$ Hz (5.9%).

Exercise ECGs belong to two different groups of subjects, volunteers and patients. The mean ± SD of the intrasubject error (μ and σ) achieved by the proposed method in each group are shown in Table I(c).

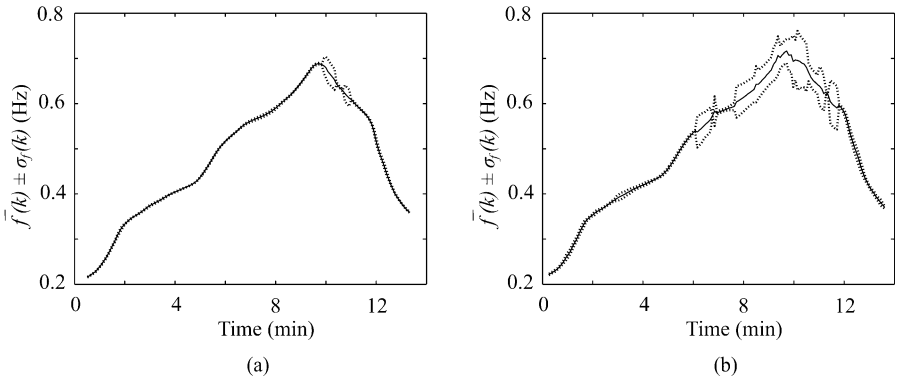

Fig. 7. Mean respiratory frequency, $\overline{f}(k)$ (solid line) $\pm\sigma_f(k)$ (dotted line), during the stress test estimated using (a) QRS-VCG loop alignment and (b) multilead QRS area techniques.

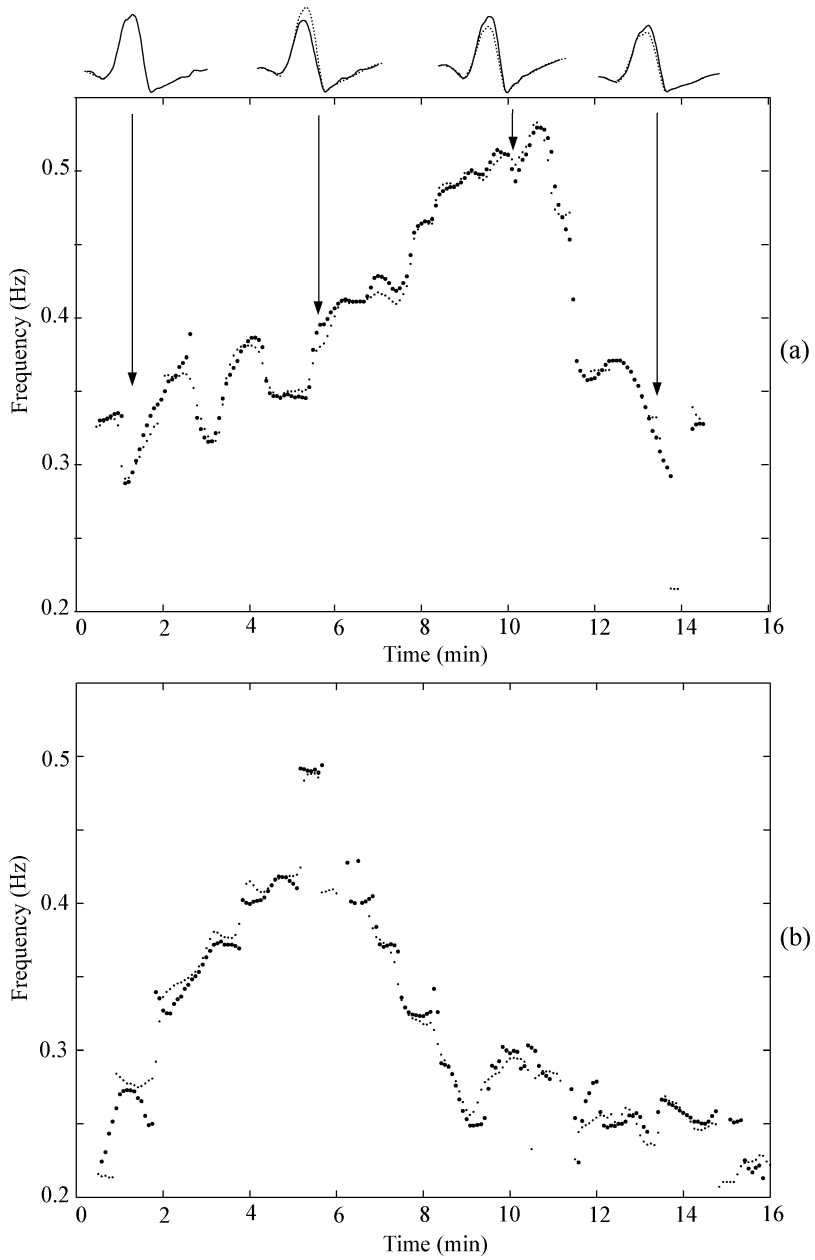

Fig. 8. Respiratory frequency estimated from the ECG $\hat{f}(k)$ (big dot) and from the respiratory signal $\hat{f}_r(k)$ (small dot) for (a) a volunteer and (b) a patient. In (a), lead X of the observed (solid line) and reference (dotted line) loop are displayed at different time instants.

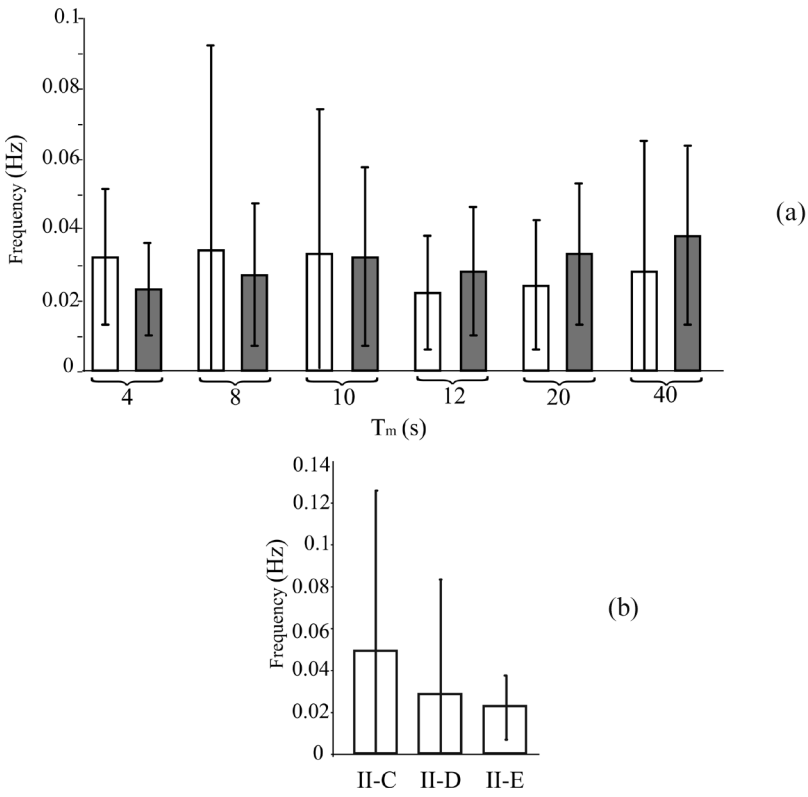

Fig. 9. (a) Mean ± SD of μ (white) and σ (gray) for different values of T_m. (b) Mean ± SD of μ for the basic method (II-C) and the two robustifying techniques sequentially introduced (II-D and II-E).

TABLE II
MEAN ± SD OF THE INTRASUBJECT ERROR FOR DIFFERENT VALUES OF T_m

T_m	4 s		8 s		10 s	
	μ	σ	μ	σ	μ	σ
Hz	0.032 ± 0.019	0.023 ± 0.013	0.034 ± 0.058	0.027 ± 0.020	0.033 ± 0.041	0.032 ± 0.025
%	8.4 ± 4.6	6.0 ± 2.7	8.4 ± 12.8	7.0 ± 4.5	8.1 ± 8.9	8.2 ± 5.1
$T_{\%}$	82±13		79±17		75±19	
T_m	12 s		20 s		40 s	
	μ	σ	μ	σ	μ	σ
Hz	0.022 ± 0.016	0.028 ± 0.018	0.024 ± 0.018	0.033 ± 0.020	0.028 ± 0.037	0.038 ± 0.025
%	5.9 ± 4.0	7.6 ± 4.1	6.3 ± 4.2	9.0 ± 4.1	7.2 ± 9.5	9.4 ± 4.6
$T_{\%}$	78±17		76±15		72±14	

VI. DISCUSSION

Several methods have exploited the idea of retrieving respiratory information from the fluctuations of the heart's electrical axis [7]–[19]. It was concluded that the orthogonal X, Y, and Z leads are better for estimating the respiratory frequency than a subset of leads [18]. In fact, the method based on the QRS-VCG loop alignment estimated the respiratory frequency of 20 healthy subjects more accurately than did the multilead QRS area method, achieving a gross median estimation error of 4.2% versus 13%. This result agrees with ours since the mean intrasubject error is $\mu = 0.002 \pm 0.001$ Hz ($0.5\% \pm 0.2\%$) using QRS-VCG loop alignment versus $\mu = 0.005 \pm 0.004$ Hz ($1\% \pm 0.7\%$) using the multilead QRS area approach in the simulation study. For exercise ECGs, the corresponding results are $\mu = 0.022 \pm 0.016$ Hz ($5.9\% \pm 4\%$) versus $\mu = 0.076 \pm 0.087$ Hz ($18.8\% \pm 21.7\%$). The QRS-VCG loop alignment estimation error reported in [18], 4.2%, is lower than the one achieved in this study, 5.9%. The reason is that the recordings of the database in [18] were from resting conditions while in this work from stress testing. There are different characteristics of stress testing recordings which make the method's performance deteriorate with respect to resting recordings and which have motivated this work: stress testing recordings are noisier than resting recordings, QRS morphology suffers exercise-induced variations which have to be compensated for, respiratory frequency is not constant during stress testing and, moreover, the respiratory unimodal pattern, common in resting conditions, is sometimes lost during exercise.

A major difference between the present method and the one in [18] is the exponentially updated reference loop $\mathbf{Y_R}(i)$ which accounts for exercise-induced morphologic QRS variations. Since the original multilead QRS area method does not compensate for such variations, the final part of the QRS

complex is excluded by analyzing only the time interval from 60 ms before to 20 ms after the QRS detection mark. Using the same time interval as for the QRS-VCG loop alignment approach, i.e., 120 ms centered around the QRS detection mark, the performance would deteriorate ($\mu = 0.025$ Hz (4.9%) in the simulated data and $\mu = 0.103$ Hz (25.2%) in exercise ECGs).

It has been shown that QRS-VCG loop alignment exhibits more robust performance than multilead QRS area especially during the latter phase of exercise, which is due to a higher robustness against noise and to a better compensation In this paper, spectral analysis is performed using Lomb's method since the angle trends are unequally spaced. Simple interpolation of the angle trends would inappropriately suppress the HF content and mask the respiratory frequency [33]. The spectra of the three angle trends are summed to account for electrical axis rotation projections on any of the leads, motivated by the fact that respiratory rotation is often more pronounced around one of the leads not "*a priori*" known. Moreover, spectral averaging is necessary to enhance the peak of the respiratory frequency, especially when spurious peaks are present. A search for the largest spectral peak in a restricted interval around the anticipated reference frequency further decreases the risk of identifying a spurious peak as the respiratory frequency. As a consequence, only limited variations in respiratory frequency can be tracked. In this paper, variations of up to 0.2 Hz per 5 s can be tracked which appears to be sufficient in stress testing.or exercise-induced morphologic QRS variations.

A method to reject outlier angle estimates was proposed in [28], which only estimated the angles from diagonally dominant rotation matrices. The value of τ which minimized ε in (1), conditioned on that the rotation matrix $\hat{\mathbf{Q}}_\tau$ was diagonally dominant, was used to estimate the EDR signal. However, this criterion turns out to be insufficient to reject outlier angle estimates, motivating the introduction of the more restrictive criterion of Section II-D. The mean intrasubject error achieved using the criterion in [28] instead of the criterion of Section II-D is of $\mu = 0.035 \pm 0.055$ Hz (8.5% $\pm$ 11.6%), in comparison to $\mu = 0.022 \pm 0.016$ Hz (5.9% $\pm$ 4%).

The results from simulated and exercise ECGs call for certain observations. The estimation errors are much larger in exercise ECGs than in simulated ECGs, $\mu = 0.022 \pm 0.016$ Hz (5.9% $\pm$ 4%) versus $\mu = 0.002 \pm 0.001$ Hz (0.5% $\pm$ 0.2%). The robustifying techniques improve performance notably in exercise ECGs but not in simulated ECGs, although nonstationary noise is added and different ST/HR patterns introduced. One reason is the underlying assumption of a respiratory spectrum with a dominant peak which is always fulfilled in simulated ECGs (respiration effect is simulated by a sigmoidal function with a clearly defined dominant frequency for each instant) but not in exercise ECGs. The respiratory signal exhibits a spectrum with more peaks, especially during exercise, where it is sometimes difficult to estimate the dominant frequency; this is the motivation for using average spectral estimation of shorter windows. At the expense of losing accuracy in the estimation of the respiratory frequency, the gross position of the respiratory frequency can be obtained. Another explanation to the differences between the results from simulated and exercise ECGs may be the deterministic nature of the ECG in the simulated data which does not account for the presence of ectopic beats. Such beats must be identified and discarded in exercise ECGs, thus reducing the sampling rate of the estimated rotation angle series.

In this paper, exercise ECGs from two different groups of subjects, volunteers and patients, have been used. The mean intrasubject error in the volunteers, $\mu = 0.016 \pm 0.009$ Hz (4.7% $\pm$ 2.9%), is lower than in the patients, $\mu = 0.028 \pm 0.018$ Hz (7.0% $\pm$ 4.7%). One reason may be that the respiratory signal exhibits a unimodal pattern (respiratory spectrum with a clearly defined dominant frequency) more often in the volunteers than in the patients, as suggested by the value of the parameter $T_{\%}$ (82% $\pm$ 15% in the volunteers and 75% $\pm$ 17% in the patients) and in the exclusion criteria (see Section III-A).

Although several methods have been developed to extract respiratory information from the ECG, very few of them are able to handle the poor SNR of exercise ECGs. In [10], a method based on QRS areas was applied to exercise ECGs (at 2×, 3×, and 4× the resting metabolic rate). The ECG-derived respiratory frequency and the frequency obtained from impedance pneumography respiratory signals did not differ with statistical significance. In [23], a different approach to predict respiratory frequency during pyramidal exercise was presented, based on the RR interval series analysis using an adaptive AR model-based method to track the respiratory frequency. The method was only applied to two subjects, and, therefore, its overall performance cannot be judged. In [19], the first principal component of a set of parameters, composed of the center of gravity and the inertial axis of successive QRS-VCG loops, was used as an estimation of the EDR signal. The correlation with simultaneous respiratory recording was high for the 4 analyzed subjects. Different situations, including a 2-min epoch of stepping, were considered. In this paper, the respiratory frequency from a total of 29 exercise ECGs is successfully derived, suggesting that the method is robust in the presence of nonstationary signals, noise, and respiratory frequency. Quantitative results of the error in estimating the respiratory frequency with respect to the one obtained from a simultaneous airflow-based respiratory signal are given, being within the range of the respiratory frequency short-term variability.

In this study, we have found two main sources of errors which are difficult to distinguish from each other: inaccurate estimates due to high levels of noise and multimodal respiratory patterns. Some approaches have been proposed in this paper to deal with the first one, while the second one may be addressed by comparing multimodal spectra with approaches like, e.g., spectral coherence.

In this paper, we have not made a distinction between learning and testing but tuned parameters to the database; therefore, parameter values may not be the optimum for other types of signals different from cycling stress testing.

Not even the recording of the respiratory signal is without problems during stress testing, and, therefore, other sensors, less sensitive to body movements than the thermistor, should be investigated to obtain the respiratory reference. The pneumotachometer, often used in exercise physiology studies, and the plethysmograph represent alternatives.

VII. Conclusion

The present method represents a powerful approach to estimation of the respiratory frequency from exercise ECGs and requires no additional equipment. The present method retrieves the respiratory frequency from exercise ECGs with a mean error of $\mu = 0.022 \pm 0.016$ Hz ($5.9\% \pm 4\%$), which is of the same order of magnitude as the short-term variability of the respiratory frequency itself, i.e. $\mu_r = 0.019 \pm 0.007$ Hz ($5.2\% \pm 1.9\%$).

Acknowledgment

The authors are very grateful to Dr. O. Pahlm and M. Nilsson, Department of Clinical Physiology, Lund University Hospital, Sweden, for their collaboration in the recording of the stress test data, and to Dr. P. Serrano, University Hospital "Lozano Blesa" of Zaragoza, Spain, for his collaboration in the recording of the data used in the simulation study.

References

[1] R. Bailón, J. Mateo, S. Olmos, P. Serrano, J. García, A. del Río, I. Ferreira, and P. Laguna, "Coronary artery disease diagnosis based on exercise electrocardiogram indexes from repolarisation, depolarisation and heart rate variability," *Med. Biol. Eng. Comput.*, vol. 41, pp. 561–571, 2003.

[2] W. Einthoven, G. Fahr, and A. Waart, "On the direction and manifest size of the variations of potential in the human heart and on the influence of the position of the heart on the form of the electrocardiogram," *Am. Heart J.*, vol. 40, pp. 163–193, 1950.

[3] J. Flaherty, S. Blumenschein, A. Alexander, R. Gentzler, T. Gallie, and J. Boineau *et al.*, "Influence of respiration on recording cardiac potentials," *Am. J. Cardiol.*, vol. 20, pp. 21–28, 1967.

[4] H. Riekkinen and P. Rautaharju, "Body position, electrode level and respiration effects on the Frank lead electrocardiogram," *Circ.*, vol. 53, pp. 40–45, 1976.

[5] P. Grossman and K. Wientjes, "Respiratory sinus arrhythmia and parasympathetic cardiac control: some basic issues concerning quantification, applications and implications," in *Cardiorespiratory and Cardiosomatic Psycophysiology*, P. Grossman, K. Jansenn, and D. Waitl, Eds. New York: Plenum, 1986, pp. 117–138.

[6] R. Pallás-Areni, J. Colominas-Balagué, and F. Rosell, "The effect of respiration-induced heart movements on the ECG," *IEEE Trans. Biomed. Eng.*, vol. 36, no. 6, pp. 585–590, Jun. 1989.

[7] R. Wang and T. Calvert, "A model to estimate respiration from vectorcardiogram measurements," *Ann. Biomed. Eng.*, vol. 2, pp. 47–57, 1974.

[8] F. Pinciroli, R. Rossi, and L. Vergani, "Detection of electrical axis variation for the extraction of respiratory information," in *Proc. Computers in Cardiology*, 1986, pp. 499–502.

[9] G. Moody, R. Mark, A. Zoccola, and S. Mantero, "Derivation of respiratory signals from multi-lead ECGs," in *Proc. Computers in Cardiology*, 1986, pp. 113–116.

[10] L. Zhao, S. Reisman, and T. Findley, "Derivation of respiration from electrocardiogram during heart rate variability studies," in *Proc. Computers in Cardiology*, 1994, pp. 53–56.

[11] D. Dobrev and I. Daskalov, "Two-electrode telemetric instrument for infant heart rate and apnea monitoring," *Med. Eng. Phys.*, vol. 20, pp. 729–734, 1998.

[12] A. Travaglini, C. Lamberti, J. de Bie, and M. Ferri, "Respiratory signal derived from eight-lead ECG," in *Proc. Computers in Cardiology*, 1998, vol. 25, pp. 65–68.

[13] B. Raymond, R. Cayton, R. Bates, and M. Chappell, "Screening for obstructive sleep apnoea based on the electrocardiogram—the computers in cardiology challenge," in *Proc. Computers in Cardiology*, 2000, vol. 27, pp. 267–270.

[14] C. Mason and L. Tarassenko, "Quantitative assessment of respiratory derivation algorithms," in *Proc. 23rd Ann. IEEE EMBS Int. Conf.*, Istanbul, Turkey, 2001, pp. 1998–2001.

[15] K. Behbehani, S. Vijendra, J. Burk, and E. Lucas, "An investigation of the mean electrical axis angle and respiration during sleep," in *Proc. 2nd Joint EMBS/BMES Conf.*, Houston, TX, 2002, pp. 1550–1551.

[16] W. Yi and K. Park, "Derivation of respiration from ECG measured without subject's awareness using wavelet transform," in *Proc. 2nd Joint EMBS/BMES Conf.*, Houston, TX, 2002, pp. 130–131.

[17] P. Chazal, C. Heneghan, E. Sheridan, E. Reilly, P. Nolan, and M. O'Malley, "Automated processing of single-lead electrocardiogram for the detection of obstructive sleep apnoea," *IEEE Trans. Biomed. Eng.*, vol. 50, no. 6, pp. 686–696, Jun. 2003.

[18] S. Leanderson, P. Laguna, and L. Sörnmo, "Estimation of the respiratory frequency using spatial information in the VCG," *Med. Eng. Phys.*, vol. 25, pp. 501–507, 2003.

[19] A. Bianchi, G. Pinna, M. Croce, M. L. Rovere, R. Maestri, E. Locati, and S. Cerutti, "Estimation of the respiratory activity from orthogonal ECG leads," in *Proc. Computers in Cardiology*, 2003, vol. 30, pp. 85–88.

[20] M. Varanini, M. Emdin, F. Allegri, M. Raciti, F. Conforti, A. Macerata, A. Taddei, R. Francesconi, G. Kraft, A. L'Abbate, and C. Marchesi, "Adaptive filtering of ECG signal for deriving respiratory activity," *Proc. Computers in Cardiology*, pp. 621–624, 1990.

[21] B. Pilgram and M. Renzo, "Estimating respiratory rate from instantaneous frequencies of long term heart rate tracings," *Proc. Computers in Cardiology*, pp. 859–862, 1993.

[22] M. Varanini, G. D. Paolis, M. Emdin, A. Macerata, S. Pola, M. Cipriani, and C. Marchesi, "Spectral analysis of cardiovascular time series by the S-transform," in *Proc. Computers in Cardiology*, 1997, vol. 24, pp. 383–386.

[23] O. Meste, G. Blain, and S. Bermon, "Analysis of the respiratory and cardiac systems coupling in pyramidal exercise using a time-varying model," in *Proc. Computers in Cardiology*, 2002, vol. 29, pp. 429–432.

[24] T. Young and W. Huggins, "The intrinsic component theory of electrocardiography," *IEEE Trans. Biomed. Eng.*, vol. BME-9, pp. 214–221, Sep. 1962.

[25] B. Mazzanti, C. Lamberti, and J. de Bie, "Validation of an ECG-derived respiration monitoring method," in *Proc. Computers in Cardiology*, 2003, vol. 30, pp. 613–616.

[26] L. Edenbrandt and O. Pahlm, "Vectorcardiogram synthesized from a 12-lead ECG: superiority of the inverse Dower matrix," *J Electrocardiol.*, vol. 21, no. 4, pp. 361–367, 1988.

[27] L. Sörnmo, "Vectorcardiographic loop alignment and morphologic beat-to-beat variability," *IEEE Trans. Biomed. Eng.*, vol. 45, no. 12, pp. 1401–1413, Dec. 1998.

[28] M. Åström, J. García, P. Laguna, O. Pahlm, and L. Sörnmo, "Detection of body position changes using the surface ECG," *Med. Biol. Eng. Comput.*, vol. 41, no. 2, pp. 164–171, 2003.

[29] N. R. Lomb, "Least-squares frequency analysis of unequally spaced data," *Astrophys. Space Sci.*, vol. 39, pp. 447–462, 1976.

[30] G. Borg, "Psychophysical bases of perceived exertion," *Med. Sci. Sports Exerc.*, vol. 14, pp. 377–381, 1982.

[31] L. Edenbrandt, A. Houston, and P. Macfarlane, "Vectorcardiograms synthesized from 12-lead ECGs: a new method applied in 1792 healthy children," *Pediatr. Cardiol.*, vol. 15, pp. 21–26, 1994.

[32] M. Åström, E. Carro, L. Sörnmo, P. Laguna, and B. Wohlfart, "Vectorcardiographic loop alignment and the measurement of morphologic beat-to-beat variability in noisy signals," *IEEE Trans. Biomed. Eng.*, vol. 47, no. 4, pp. 497–506, Apr. 2000.

[33] C. Birkett, M. Kienzle, and G. Myers, "Interpolation over ectopic beats increases low frequency power in heart rate variability spectra," in *Proc. Computers in Cardiology*, 1992, pp. 257–259.

Raquel Bailón was born in Zaragoza, Spain, in 1978. She received the M.Sc. degree in telecommunications engineering from the University of Zaragoza (UZ) in 2001. In 2001, she started working towards the Ph.D. degree at the Department of Electronic Engineering and Communications, UZ, with a grant supported by the Spanish government.

Since 2003, she is an Assistant Professor in the same department. Her main research activity lies in the field of biomedical signal processing, especially in the analysis of the electrocardiogram for diagnosis purposes

Leif Sörnmo (S'80–M'85–SM'02) received the M.Sc. and Ph.D. degrees in electrical engineering from Lund University, Lund, Sweden, in 1978 and 1984, respectively.

He held a research position with the Department of Clinical Physiology, Lund University, from 1983 to 1995, where he worked on computer-based ECG analysis. Since 1990, he has been with the Signal Processing Group, Department of Electroscience, Lund University, where he now holds a position as a Professor in biomedical signal processing. His main research interests include statistical signal processing and modeling of biomedical signals. His current research projects include methods in ischemia monitoring, time-frequency analysis of atrial fibrillation, power efficient signal processing in pacemakers, hemodialysis, and detection of otoacoustic emissions. He is, together with P. Laguna, the author of *Bioelectrical Signal Processing in Cardiac and Neurological Applications* (Elsevier, 2005).

Dr. Sörnmo has been an Associate Editor of *Computers in Biomedical Research* (1997–2000). He is currently on the editorial boards of the IEEE TRANSACTIONS ON BIOMEDICAL ENGINEERING, the *Journal of Electrocardiology,* and *Medical and Biological Engineering & Computing*.

Pablo Laguna (M'92–SM'06) was born in Jaca (Huesca), Spain, in 1962. He received the Physics degree (M.S.) and the Doctor in Physic Science degree (Ph.D.) from the Science Faculty at the University of Zaragoza, Zaragoza, Spain, in 1985 and 1990, respectively. The Ph.D. thesis was developed at the Biomedical Engineering Division of the Institute of Cybernetics (U.P.C.-C.S.I.C.) under the direction of P. Caminal.

He is Full Professor of Signal Processing and Communications in the Department of Electrical Engineering at the Engineering School, and a Researcher at the Arag\'on Institute for Engineering Research (I3A), both at University of Zaragoza, Spain. From 1992 to 2005, was Associated Professor at same university and from 1987 to 1992 he worked as Assistant Professor of Automatic Control in the Department of Control Engineering at the Politechnic University of Catalonia (U.P.C.), Catalonia, Spain, and as a Researcher at the Biomedical Engineering Division of the Institute of Cybernetics (U.P.C.-C.S.I.C.). His professional research interests are in signal processing, in particular applied to biomedical applications. He is, together with L. Sörnmo, the author of *Bioelectrical Signal Processing in Cardiacand Neurological Applications* (Elsevier, 2005).